Digital Signal Processing 73 (2018) 16–23

Contents lists available at ScienceDirect

Digital Signal Processing

www.elsevier.com/locate/dsp

Mixed near-field and far-field source localization utilizing symmetric nested array

Ye Tian [a,b,*], Qiusheng Lian [a], He Xu [a]

[a] School of Information Science and Technology, Yanshan University, Qinhuangdao, Hebei, 066004, China
[b] CETC Key Laboratory of Aerospace Information Applications, Shijiazhuang, Hebei, 050081, China

ARTICLE INFO

Article history:
Available online 6 November 2017

Keywords:
Mixed source localization
Near-field sources
Far-field sources
Symmetric nested array
Fourth-order cumulant

ABSTRACT

Existing mixed near-field and far-field source localization algorithms rely on uniform linear array (ULA), and the maximum number of sources that they can detect is less than the sensor number. As a comparison, recently proposed nested array can provide higher number of consecutive lags with the same sensor number, enabling us to extend it to mixed source localization scenario. Instead of utilizing generalized nested array, we design a symmetric nested array (SNA) for mixed source localization. By constructing a fourth-order cumulant matrix that only related to DOA information, the newly designed symmetric nested array exhibits at least of $4N + 4MN - 2M - 3$ consecutive lags with only $2M + 2N - 1$ sensors. A compressive sensing (CS) based approach is exploited to achieve DOA estimation of all sources by fully using these consecutive lags. Based on the estimated DOAs, the range of near-field sources is obtained by 1-D spectral search, and the near-field and far-field sources are classified successively in range domain. By conducting numerical simulations, we show the superiority of the proposed algorithm in terms of estimation accuracy, number of required array sensors, and resolution ability compared with previous algorithms.

1. Introduction

In the last few decades, research on far-field and near-field source localization has received a widespread amount of attention, and various algorithms have been developed for dealing with these two issues, examples include MUSIC [1] and ESPRIT [2] algorithms for far-field source localization, 2-D MUSIC-smooth [3] and path following [4] algorithms for near-field source localization. When the location of a source is far beyond the Fresnel region [5], only direction-of-arrival (DOA) information is required. In contrast, when a source is located close to the array, both DOA and range (the distance between the array and the source) parameters are required to characterize the wavefront. So far, the pure far-field and pure near-field source localization problems have been well solved. However, in some practical applications, such as speaker localization using microphone arrays and guidance systems [6–8], near-field and far-field sources may exist simultaneously. In these situations, the above mentioned algorithms may fail in locating and classifying the mixed sources.

Recently, as locating mixed near-field and far-field sources become more and more attractable, several researchers have attempted to propose some suitable algorithms for mixed source localization scenario. By constructing two special fourth-order cumulant matrices, a two-stage MUSIC (TS-MUSIC) algorithm [9] is presented to solve the mixed source localization problem, whose key concept is to estimate the DOAs of all sources first, and then distinguish the mixed sources via 1-D spectral search in range domain. That is, if the spectral peak appears in the Fresnel region, we can judge that it is a near-field source. On contrast, if the spectral peak appears far beyond the Fresnel region, we can judge that it is a far-field source. Based on this concept, references [10,11] and [12] respectively apply Group Lasso (G-Lasso), Lasso and ESPRIT-Like techniques for mixed source localization, and successively provide improved resolution and estimation accuracy in comparison with TS-MUSIC. Differ from TS-MUSIC, He et al. [13] and Liu et al. [14] propose another strategy for mixed source localization, where the DOAs of far-field sources are first estimated by 1-D spectral search, then the oblique projection technique and spatial differencing technique (a technique that exploits the eigenstructure differences between the far-field covariance matrix and the near-field one) are respectively exploited to suppress the influence of far-field sources. Finally, the DOA and range parameters related to near-field sources are well obtained.

Although the existing algorithms mentioned above can work in mixed near-field and far-field source scenario, the maximum num-

* Corresponding author.
E-mail address: tianye@ysu.edu.cn (Y. Tian).

https://doi.org/10.1016/j.dsp.2017.10.021
1051-2004/

ber of consecutive lags is not adequate since the array structure utilized is uniform linear array (ULA). As is well know, the maximum number of consecutive lags provided by ULA with P sensors is typically $2P-1$ and the maximum number of sources that it can detect is usually less than the sensor number. However, the problem of estimating more sources with less sensors is of tremendous interest in various applications [15,16]. Toward this purpose, several nonuniform linear arrays, such as nested array (obtained by systematically nesting two or more uniform linear arrays) [17] and co-prime array (obtained by utilizing a coprime pair of uniform linear subarrays) [18], are designed. These kind of array configurations can increase the number of consecutive lags greatly. In particular, the nested array is easy to construct and it is possible to obtain the available consecutive lags for a given number of sensors.

Inspired by the idea of nonuniform array, this paper first expands the general nested array to the symmetrical form, and then applies it to mixed source localization. By constructing two fourth-order cumulant matrices of properly chosen sensor outputs, the designed symmetric nested array (SNA) exhibits larger number of consecutive lags than the ULA under the same sensor number. Similar to the concept of TS-MUSIC, we first estimate the DOAs of all sources, and then obtain the range estimation of near-field sources via 1-D spectral search, as well as distinguish the mixed sources in range domain. The differences between the TS-MUISC in [9] and the present work can be summarized as three points: 1) The DOAs of all sources are estimated by CS-based approach instead of subspace technique in our work, which can lead to better resolution and noise robustness. 2) Instead of using ULA, SNA is designed and exploited in our work, as a result, the number of sources that it can detect is increased greatly. 3) Our work is applicable to the case where far-field and near-field sources impinging on the array with same DOAs. The final result is in the sense that an improved mixed source localization performance is provided by our work.

The paper is organized as follows: In Section 2, we introduce the mixed near-field and far-field signal model, where the symmetric nested array is adopted. In Section 3, we first analyze the characteristic of SNA in fourth-order cumulant domain, and then propose the new mixed source localization and classification algorithm. Section 4 presents extensive numerical simulations to show the advantages of our algorithm in terms of estimation accuracy, maximum number of sources that it can detect, and resolution ability. Section 5 draws the conclusion of the whole paper.

Notations: We use bold capital letters ($\mathbf{A}$, $\mathbf{A}_m$ etc.) for matrices, bold small case letters ($\mathbf{x}$, $\mathbf{x}_m$ etc.) for vectors and non-bold letters (m, G etc.) for scalars. The superscripts T, $*$ and H imply the transpose, complex conjugate and conjugate transpose, respectively. vec$(\cdot)$ represents the vectorization operation that turns a matrix into a vector by stacking all columns on top of the another, and $\mathbf{r}^N$ denotes a feasible set with N components. $\|\cdot\|_2$ and $\|\cdot\|_1$ respectively denote the ℓ_2-norm and ℓ_1-norm, and $\lceil\cdot\rceil$ is the ceiling operator. $\otimes$ denotes the Kronecker product, and diag(c_1, c_2) denotes a diagonal matrix with diagonal entries c_1 and c_2. In particular, the fourth-order cumulants can be arranged in the form of cumulant matrices in two different ways. These matrices are indexed by l $(=1,2)$, and denoted as $\mathbf{C}_{4,\mathbf{x}}(l)$.

2. Signal model

Suppose that K narrow-band and uncorrelated signal waveforms, generated by near-field and far-field sources, impinging on a SNA with $2M+2N-1$ omnidirectional sensors, as depicted in Fig. 1. It contains two parts, part1 is a ULA with inter-sensor spacing d, and part2 is another ULA with inter-sensor spacing $(2N-1)d$, where d represents the unit spacing. The distance between two parts is also $(2N-1)d$. If we use D to represent the set of sensor positions, then we have

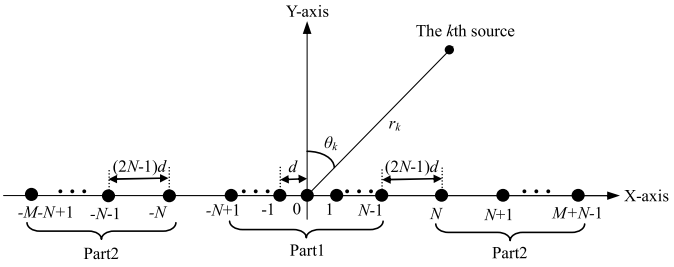

Fig. 1. The symmetric nested array configuration.

$$D=\{p_{-L}\cdot d,\cdots,p_0\cdot d,\ldots,p_L\cdot d\} \tag{1}$$

where $L=M+N-1$, $p_i\cdot d$ is the position of ith sensor, $i\in[-L,L]$. The value of p_i is defined as follows

$$p_i=\begin{cases} i, & |i|\le N-1 \\ (2N-1)i-2(N-1)^2, & N\le|i|\le L. \end{cases} \tag{2}$$

Let the center of array be the phase reference point, after sampled with a proper frequency that satisfies the Nyquist theorem, the signal received by the ith sensor can be expressed as

$$x_i(t)=\sum_{k=1}^{K}s_k(t)e^{j\tau_{ik}}+n_i(t),\quad t=1,\cdots,Q \tag{3}$$

where $s_k(t)$ is the kth source signal, $n_i(t)$ is the additive noise embedded in ith sensor, Q denotes the number of snapshots, and τ_{ik} indicates the propagation time delay of k source arriving at ith sensor with respect to the 0th one. If the kth source is a far-field one, τ_{ik} has the following form

$$\tau_{ik}=p_i\gamma_k \tag{4}$$

where $\gamma_k=-2\pi d\sin(\theta_k)/\lambda$, and θ_k, λ represent the DOA of kth source and the carrier wavelength, respectively. If the kth source is a near-field one, then by using the Taylor expansion [19], τ_{ik} can be approximately expressed as

$$\tau_{ik}=p_i\gamma_k+{p_i}^2\phi_k \tag{5}$$

where $\phi_k=\pi d^2\cos^2/(\theta_k)/\lambda r_k$, r_k represents the range of kth source.

Assume that there are K_1 near-field sources and $K-K_1$ far-field sources. Consequently, the vector form of (3) can be written as

$$\mathbf{x}(t)=\mathbf{A}_N\mathbf{s}_N(t)+\mathbf{A}_F\mathbf{s}_F(t)+\mathbf{n}(t) \tag{6}$$

where

$$\mathbf{x}(t)=\left[x_{-L}(t),\ldots,x_0(t),\ldots,x_L(t)\right]^T \tag{7}$$

$$\mathbf{n}(t)=\left[n_{-L}(t),\cdots,n_0(t),\ldots,n_L(t)\right]^T \tag{8}$$

$$\mathbf{A}_N=\left[\mathbf{a}(\theta_1,r_1),\ldots,\mathbf{a}(\theta_{K_1},r_{K_1})\right] \tag{9}$$

$$\mathbf{A}_F=\left[\mathbf{a}(\theta_{K_1+1}),\ldots,\mathbf{a}(\theta_K)\right] \tag{10}$$

$$\mathbf{s}_N(t)=\left[s_1(t),\cdots,s_{K_1}(t)\right]^T \tag{11}$$

$$\mathbf{s}_F(t)=\left[s_{K_1+1}(t),\cdots,s_K(t)\right]^T \tag{12}$$

and $\mathbf{a}(\theta,r)=[e^{j(p_{-L}\gamma+p_{-L}^2\phi)},\ldots,1,\ldots,e^{j(p_L\gamma+p_L^2\phi)}]^T$, $\mathbf{a}(\gamma)=[e^{jp_{-L}\gamma},\ldots,1,\ldots,e^{jp_L\gamma}]^T$ denote the steering vector of near-field source and far-field source respectively, $\gamma=-2\pi d\sin(\theta)/\lambda$, $\phi=\pi d^2\cos^2(\theta)/\lambda r$.

Throughout the paper, the following hypotheses are required to hold:

- The source signals are statistically independent, zero-mean random process with nonzero kurtosis;
- The sensor noise is the additive Gaussian white one, and independent from the source signals;
- The sensor array is a SNA with unit inter-sensor spacing $d \leq \lambda/4$, and the number of sources satisfies $K \leq 2N+2MN-M-2$, where $N>1, M>0$;
- There is no mutual coupling or the mutual coupling has been pre-compensated by calibration methods, such as the method of moment (MoM) [20] or the receiving mutual impedance method (RMIM) [21].

3. The proposed algorithm

3.1. Analysis the characteristic of SNA in cumulant domain

Fourth-order cumulant can provide increased number of consecutive lags for an array with given sensor number [22], thus it is chosen as a key technique for mixed source localization in this paper. By definition, the fourth-order cumulant of the array output can be expressed as

$$\begin{aligned}&\operatorname{cum}\left\{x_m(t), x_n^*(t), x_\rho(t), x_q^*(t)\right\}\\&=\sum_{k=1}^{K} c_{4,s_k} e^{j[(p_m-p_n+p_\rho-p_q)\gamma_k+(p_m^2-p_n^2+p_\rho^2-p_q^2)\phi_k]}\end{aligned} \tag{13}$$

where $m,n,\rho,q\in[-L,L]$, and c_{4,s_k} is the kurtosis of the kth signal.

To realize mixed source localization and avoid estimation failure problem, an intelligent strategy is to estimate DOAs of all sources without the influence of range parameter, which has been exploited by several literatures, such as [9–11]. Therefore, we need $m=-n$ and $\rho=-q$, which leads to

$$\operatorname{cum}\left\{x_m(t), x_{-m}^*(t), x_{-q}(t), x_q^*(t)\right\}=\sum_{k=1}^{K} c_{4,s_k} e^{j(p_m-p_q)2\gamma_k}. \tag{14}$$

It is easily observed that Eq. (14) is only related to DOA parameter, which provides a possible way for us to achieve DOA estimation of all sources first.

Proposition 1. *Let $\mathbb{L}=\{l_c | l_c=p_m-p_q\}$ denote the SNA lags in cumulant domain, where $-L\leq m\leq L$, $-L\leq q\leq L$. The following facts hold for the SNA:*

(a) *There are at least $4N+4MN-2M-3$ consecutive lags in $\mathbb{L}$ with the range $[-2N-2MN+M+2, 2N+2MN-M-2]$;*
(b) *The maximum number of consecutive lags can be achieved with $N=\lceil\frac{2L+3}{4}\rceil$ or $M=\lceil\frac{2L-3}{4}\rceil$, where $\lceil\cdot\rceil$ denotes the ceiling operation.*

Proof. (a) We prove it using stepwise strategy. For two arbitrary integers satisfying $|m|\leq N-1$, $|q|\leq N-1$, we have $l_{c1}(m,q)=p_m-p_q=m-n$, from which we can easily obtain that there are $4N-3$ consecutive lags with the subrange $\mathbb{L}_1=[-2N+2, 2N-2]$.

If $N\leq m\leq L-1$ and $|q|\leq N-1$, we have

$$l_{c2}(m,q)=p_m-p_q=(2N-1)\times m-2(N-1)^2-q. \tag{15}$$

Consequently, the following relationships hold

$$l_{c2}(N,q)=3N-2-q\in[2N-1, 4N-3] \tag{16}$$

$$l_{c2}(m+1,N-1)-l_{c2}(m,-N+1)=1 \tag{17}$$

$$l_{c2}(L,-N+1)=2MN+2N-M-2 \tag{18}$$

which mean that there exists $2MN-M$ consecutive lags with the subrange $\mathbb{L}_2=[2N-1, 2MN+2N-M-2]$.

Similarly, $-L\leq m\leq -N$ and $|q|\leq N-1$ will lead to another $2MN-M$ consecutive lags with the subrange $\mathbb{L}_3=[-2MN-2N+M+2, -2N+1]$.

Note that if both $N\leq|m|\leq L$, $N\leq|p|\leq L$, we will obtain $2(L-N)$ different lags with interval $2N-1$, but its continuity with $\mathbb{L}_1$, $\mathbb{L}_2$ and $\mathbb{L}_3$ cannot be guaranteed.

Based on the above analysis, we can conclude that the number of consecutive lags is at least $4N+4MN-2M-3$, and its corresponding range is $[-2N-2MN+M+2, 2N+2MN-M-2]$.

(b) Define $f(N)=4N+4MN-2M-3$, where $M=L-N+1$. Derivation on N leads to

$$f'(N)=-4N^2+(4L+10)N-2(L+1)-3. \tag{19}$$

Note that N is an integer, thus it can be easily obtained that $N=\lceil\frac{2L+3}{4}\rceil$ or $M=L-N+1=\lceil\frac{2L-3}{4}\rceil$ can produce the maximum value of f.

This concludes the proof of Proposition 1. □

The number of consecutive lags indicates the number of virtual ULA sensors generated by SNA, which is identified with fixed M and N. An example is illustrated in Fig. 2 with 7 sensors in total. Fig. 2(a) and Fig. 2(b) exhibit the SNA lags with $M=N=2$ and $M=1, N=3$, respectively. Note that the maximum number of consecutive lags provided by general ULA with P $(=7)$ sensors in mixed source localization scenario is typically $2P-1=13$. Therefore, we can easily obtain from Fig. 2 that $\bar{P}$ $(=17$ or $19)$ consecutive lags mean a virtual ULA with $\frac{\bar{P}+1}{2}$ $(=9$ or $10)$ sensors, which is larger than the actual number of sensors.

Remark 1. The maximum number of consecutive lags is our major concern and is of great importance for source localization algorithm. For one thing, with an appropriate unit spacing between adjacent virtual sensors, it can be easily exploited by various existing source localization algorithms presented with ULA. For another, it clearly points out the maximum number of sources that it can detect without phase ambiguity problem. In addition, according to the cross-correlation computer theory [23], the estimation accuracy increases as the number of virtual sensors increases. Therefore, the maximum number of consecutive lags is the fundamental guidance for good estimation. Note that the maximum number of consecutive lags produced by ULA in mixed source localization scenario is typically less than the sensor number [9–14]. However, it is clear from Proposition 1 that if M and N are set properly, the maximum number of consecutive lags produced by SNA will be much higher than the sensor number.

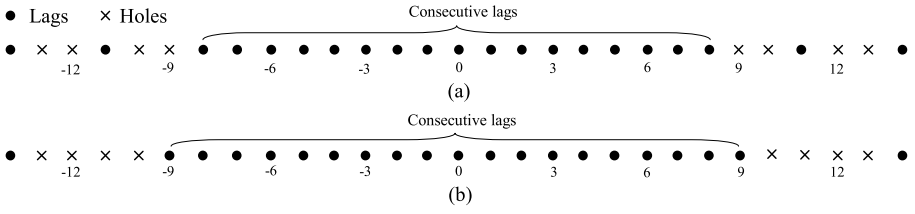

Fig. 2. An example of SNA lags. (a) $M=N=2$. (b) $M=1$, $N=3$.

Table 1
Maximum number of consecutive lags given by ULA and SNA.

Sensor number	L	M	N	Maximum number of consecutive lags	
				ULA	SNA
5	2	1	2	9	11
7	3	1	3	13	19
9	4	2	3	17	29
11	5	2	4	21	41
13	6	3	4	25	55

Table 1 is a clear comparison about the maximum number of consecutive lags produced by the ULA and SNA. As the results show, the symmetric nested structure offers the higher maximum number of consecutive lags (especially for $L \geq 4$) for DOA estimation in mixed source scenario.

3.2. DOA estimation of all sources

Let $\bar{m} = m + L + 1$, $\bar{q} = q + L + 1$, then we define the $(2L+1) \times (2L+1)$ cumulant matrix $\mathbf{C}_1$, whose $(\bar{m}, \bar{q})$th element is given by

$$\mathbf{C}_1(\bar{m}, \bar{q}) = \sum_{k=1}^{K} c_{4,s_k} e^{j(p_m - p_q)2\gamma_k}. \tag{20}$$

The matrix form of $\mathbf{C}_1$ is expressed as

$$\mathbf{C}_1 = \mathbf{B}(\theta)\mathbf{C}_S\mathbf{B}^H(\theta) = \sum_{k=1}^{K} c_{4,s_k}\mathbf{b}(\theta_k)\mathbf{b}^H(\theta_k) \tag{21}$$

where $\mathbf{C}_S = \mathrm{diag}\{c_{4,s_1}, \ldots, c_{4,s_K}\}$ denotes the signal cumulant matrix, and $\mathbf{B}(\theta) = [\mathbf{b}(\theta_1), \ldots, \mathbf{b}(\theta_K)]$ represents the steering matrix, whose kth column is given by

$$\mathbf{b}(\theta_k) = \left[e^{jp_{-L}\omega_k}, \ldots, 1, \ldots, e^{jp_L\omega_k}\right]^T, \tag{22}$$

where $\omega_k = -2\pi d_1 \sin(\theta_k)/\lambda$ with $d_1 = 2d \leq \lambda/2$.

It can be easily observed that $\mathbf{C}_1$ has the similar form with the covariance matrix obtained in pure far-field case. Therefore, $\mathbf{C}_1$ can be regarded as the virtual array output in cumulant domain, which can be directly applied for DOA estimation of mixed sources without phase ambiguity problem.

Vectorizing $\mathbf{C}_1$ in (21) yields

$$\mathbf{z} = \mathrm{vec}(\mathbf{C}_1) = \mathbf{B}_1(\theta)\mathbf{c} \tag{23}$$

where $\mathbf{B}_1(\theta) = [\mathbf{b}_1(\theta_1), \ldots, \mathbf{b}_1(\theta_K)]$, $\mathbf{b}_1(\theta_k) = \mathbf{b}^*(\theta_k) \otimes \mathbf{b}(\theta_k)$, and $\mathbf{c} = [c_{4,s_1}, \ldots, c_{4,s_K}]^T$.

Note that the virtual signal model $\mathbf{z}$ is a single snapshot, thus the subspace-based algorithms cannot be applied directly. Alternatively, we exploit the CS-approach termed Lasso [24] to achieve DOA estimation, whose objective function is defined as

$$\min\left\{(1-h)\|\mathbf{z} - \boldsymbol{\Phi}\mathbf{c}_G\|_2^2 + h\|\mathbf{c}_G\|_1\right\} \tag{24}$$

where $\boldsymbol{\Phi} = [\mathbf{b}_1(\bar{\theta}_1), \ldots, \mathbf{b}_1(\bar{\theta}_G)]$ denotes the sensing matrix, defined over a finite sampling grid $\bar{\theta}_1, \ldots, \bar{\theta}_G$, and all the vectors $\{\mathbf{b}_1(\theta_k)\}_{k=1}^K$ are included in $\boldsymbol{\Phi}$, $G \gg K$. $0 \leq \mathbf{c}_G \in \mathbb{R}^G$ is a K-sparse vector, whose gth element is non-zero if source k comes from $\bar{\theta}_g$ and zeros otherwise. h is a regularized parameter that balance the ℓ_2-norm term and ℓ_1-norm term, and selected via L-curve method [25]. From Fig. 3, we can observe that $h = 0.6$ is a good choice that corresponds to the corner in L-curve. The optimization problem (24) can be solved using some convex-type software package, such as SeDuMi [26] or CVX [27]. By finding the indexes of K largest values in $\mathbf{c}_G$, the DOAs of all sources are obtained.

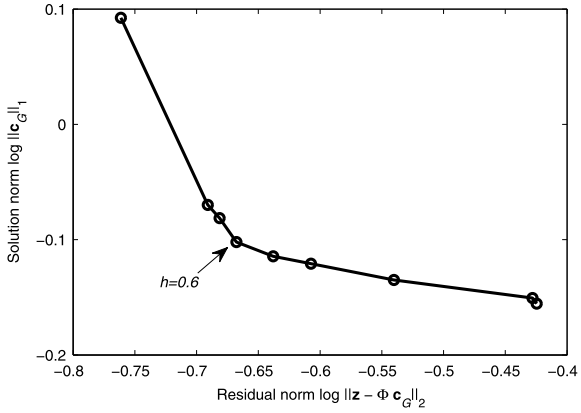

Fig. 3. The L-curve in the log–log scale.

Remark 2. We can also use the spatial smoothing MUSIC (SS-MUSIC), as described in [28], to achieve DOA estimation. However, spatial smooth not only result in certain loss of degrees of freedom, but also require element rearranging to construct a consecutive difference lag set, which we think is not an intelligent strategy. Moreover, the SS-MUSIC underperforms the CS-based approach (see the experiment for details).

3.3. Range estimation and source type classification

Since the DOAs of all sources have been successfully obtained, the main concern of this subsection is to estimate the range of near-field source and classify the source types (i.e., judging the kth source is the far-field one or the near-field one) effectively. To achieve this goal, we construct another fourth-order cumulant matrix. Under the assumption of statistically independent source signals and white Gaussian noise, the complete fourth-order cumulant matrix indexed by l $(= 1, 2)$ can be obtained by arranging the elements in an appropriate manner, whose expression is given by

$$\begin{aligned}\mathbf{C}_{4,\mathbf{x}}(l) = &\sum_{k=1}^{K_1} c_{4,s_k}[\mathbf{a}(\theta_k, r_k)^{\otimes l} \otimes \mathbf{a}(\theta_k, r_k)^{*\otimes(2-l)}] \\ &\times [\mathbf{a}(\theta_k, r_k)^{\otimes l} \otimes \mathbf{a}(\theta_k, r_k)^{*\otimes(2-l)}]^H \\ &+ \sum_{k=1}^{K-K_1} c_{4,s_k}[\mathbf{a}(\theta_k)^{\otimes l} \otimes \mathbf{a}(\theta_k)^{*\otimes(2-l)}] \\ &\times [\mathbf{a}(\theta_k)^{\otimes l} \otimes \mathbf{a}(\theta_k)^{*\otimes(2-l)}]^H.\end{aligned} \tag{25}$$

The matrix form of $\mathbf{C}_{4,\mathbf{x}}(l)$ with $l = 1$ can be given by

$$\mathbf{C}_{4,\mathbf{x}}(1) = \mathbf{D}_N(\theta, r)\mathbf{C}_{S1}\mathbf{D}_N^H(\theta, r) + \mathbf{D}_F(\theta)\mathbf{C}_{S2}\mathbf{D}_F^H(\theta) \tag{26}$$

where $\mathbf{D}_N(\theta, r) = [\mathbf{d}(\theta_1, r_1), \ldots, \mathbf{d}(\theta_{K_1}, r_{K_1})]$ with its kth column $\mathbf{d}(\theta_k, r_k) = \mathbf{a}(\theta_k, r_k) \otimes \mathbf{a}_N(\theta_k, r_k)^*$, $\mathbf{D}_F(\theta) = [\mathbf{d}(\theta_{K_1+1}), \ldots, \mathbf{d}(\theta_K)]$ with its kth column $\mathbf{d}(\theta_k) = \mathbf{a}(\theta_k) \otimes \mathbf{a}(\theta_k)^*$. Assume that the number of sources K is known or pre-estimated correctly. Implementing the eigenvalue decomposition (EVD) on $\mathbf{C}_{4,\mathbf{x}}(1)$ yields to

$$\mathbf{C}_{4,\mathbf{x}}(1) = \mathbf{E}_S\Delta_S\mathbf{E}_S^H + \mathbf{E}_n\Delta_n\mathbf{E}_n^H \tag{27}$$

where $\mathbf{E}_S$ and $\mathbf{E}_n$ denote the signal-subspace matrix and noise-subspace matrix, respectively. Δ_S is a diagonal matrix that corresponds to the K largest eigenvalues, and Δ_n is another diagonal matrix that corresponds to the $(2L+1)^2 - K$ smallest ones.

According to the result shown in [13], the DOAs of far-field sources can be estimated from the following 1-D spectral function

$$\mathrm{P}(\theta) = \left[\mathbf{d}^H(\theta)\mathbf{E}_n\mathbf{E}_n^H\mathbf{d}(\theta)\right]^{-1}. \tag{28}$$

Note that if the far-field and near-field sources impinging on the array with distinct DOAs, then mixed sources are successfully classified by combining the results obtained via (24) and (28). Without lose of generality, we let $\{\hat{\theta}_k, k = 1, \ldots, K_1\}$ denote the DOAs of near-field sources. Consequently, the range estimate of the kth near-field source can be found by

$$\hat{r}_k = \min_r \left[\mathbf{d}^H(\hat{\theta}_k, r)\mathbf{E}_n\mathbf{E}_n^H\mathbf{d}(\hat{\theta}_k, r)\right]^{-1} \tag{29}$$

where r belongs to the Fresnel region and lies in the interval $[0.62(R^3/\lambda)^{1/2}, 2R^2/\lambda]$ [10–12], and R denotes the array aperture.

However, when some of near-field sources have the same DOA with the far-field ones, $\mathbf{z}$ in (23) becomes

$$\mathbf{z} = \mathbf{B}'_1(\theta)\mathbf{c}' = \sum_{k'=1}^{\hat{K}} \mathbf{b}_1(\theta_{k'})c_{4,s_{k'}} \tag{30}$$

where $\hat{K} < K$, and $\hat{K}$ denote the number of DOAs obtained by (24). Therefore, the application of estimator (29) would yield only $\hat{K} - (K - K_1) < K_1$ range estimates. That is, the objective function (29) is invalid, and the corresponding solutions are non-robust in this case. Fortunately, this problem can be easily solved by expanding the searching scope of DOA and range to $\{\bar{\theta}_k, k = 1, \ldots, \hat{K}\}$ and $\{\mathbf{r}^N\ r_F\}$, respectively, where $\bar{\theta}_k, k = 1, \ldots, \hat{K}$, denotes the estimated DOAs of all sources obtained by (24), $\mathbf{r}^N = \{\bar{r}_1, \bar{r}_2, \ldots, \bar{r}_{\bar{N}}\} \in [0.62(R^3/\lambda), 2R^2/R^2\lambda\lambda]$ and $r_F \gg 2R^2/\lambda$ denote the range grid for near-field and far-field sources, respectively. Since the range of far-field sources tends to infinity, the range grid r_F is only the approximation of far-field situation. However, simulation results show that this approximation is a good choice for mixed source classification. In fact, the similar approach has been exploited in reference [10], and the effectiveness has also been verified efficiently. If there exist two spectral peaks that fall into $\mathbf{r}_N$ and r_F with $\bar{\theta}_k$ respectively, we can ensure that one near-field source and one far-field source impinging on the array with same DOA.

Remark 3. In practical implementation, $\hat{K} < K$ indicates that there exist some sources impinging on the array with same DOA. In this case, the searching scope must be expanded.

3.4. Discussion on required number of sensors and estimation accuracy

Based on the property of Proposition 1 and the ambiguity assumption $d \leq \lambda/4$, the minimum number of consecutive lags for the SNA is $4N+4MN-2M-3$, which means that $\min[\text{Spark}(\mathbf{\Phi})] = 4N + 4MN - 2M - 2$, where Spark$(\cdot)$ represents the smallest integer of the columns of $\mathbf{\Phi}$ that are linearly dependent. According to the unique representation theory [29], the proposed algorithm admits a unique K-sparse DOA solution only if $K <$ Spark$(\mathbf{\Phi})/2$. That is, the proposed algorithm can accomplish at least $2N + 2MN - M - 2$ sources DOA estimation with $2M + 2N - 1$ sensors. Note that the rank of the constructed matrix $\mathbf{C}_{4,\mathbf{x}}(1)$ is larger than K, therefore the range parameters can be obtained effectively via (29). As a comparison, the maximum number of sources detected by the previous mixed sources localization algorithms, such as TS-MUSIC, G-Lasso and ESPRIT-Like, is less than the sensor number (i.e., $K < 2M + 2N - 1$). In other words, the required number of sensors for the proposed algorithm is less than that of the previous algorithms, provided that K is given.

According to the cross-correlation computer theory [23], the higher number of virtual sensors will lead to the better estimation accuracy. As can be seen in Proposition 1 and Table 1, the adopted SNA provides increased number of virtual sensors in comparison with ULA, thus it can be predicted that the proposed algorithm would have better performance than that of previous algorithms.

3.5. About the Cramér–Rao lower bound

As is well known, there exist two types of Cramér–Rao Lower Bound (CRLB), termed as deterministic CRLB and stochastic CRLB. We assume the source signals to be random. Therefore, the deterministic model loses its relevance. The stochastic CRLB for mixed source localization has been investigated in [13] under the Gaussian model assumption. However, the Gaussian model is not appropriate for our case since for the Gaussian model, the corresponding fourth-order cumulant matrices are zero. Meanwhile, it should be pointed out that our algorithm is well suited for underdetermined case (i.e., source number > sensor number). Although there exist some literatures [30–32] addressing the derivation of CRLB for underdetermined case in recent years. Unfortunately, it is derived under the conventional case where the source signal is considered as deterministic or Gaussian, and the mixed sources do not coexist. Therefore, they are not applicable for our case since the assumptions do not match. The derivation of CRLB for mixed source localization and underdetermined case might as well be a topic of research in our further work.

4. Simulations

In this section, the performance of the proposed algorithm is investigated, and compared with those of TS-MUSIC algorithm [9], G-Lasso algorithm [10], ESPRIT-Like algorithm [12] and SS-MUSIC algorithm [28]. The number of sensors is set to be 7 with $M = 1, N = 3$, and the unit inter-sensor spacing $d = \lambda/4$. Each source signal is modelled as $e^{j\zeta_t}$, where the phase ζ_t are uniformly distributed in $[0, 2\pi]$. The signal-to-noise ratio (SNR) and the root mean square error (RMSE) are respectively defined as

$$SNR = 10\lg \frac{E\{\mathbf{s}(t)\mathbf{s}^H(t)\}}{E\{\mathbf{n}(t)\mathbf{n}^H(t)\}} \tag{31}$$

$$RMSE = \sqrt{\frac{1}{VK}\sum_{k=1}^{K}\sum_{v=1}^{V}(\tilde{\alpha}_{kv} - \alpha_k)^2} \tag{32}$$

where $\mathbf{s}(t) = [s_1(t), \ldots, s_K(t)]^T$, K and V represent the number of sources and Monte-Carlo trials, respectively. $\tilde{\alpha}$ is the estimation result of localization parameters (DOA or range), and α denotes the true ones. In the following experiments, the RMSE and the probability of separation that indicate the performance of the proposed algorithm are obtained by 300 independent Monte-Carlo trials.

In the first experiment, we examine the ability of the proposed algorithm to distinguish the maximum number of sources. A sufficient number of snapshots obtained by 20 times sampling ratio, fixed at 10000, is utilized for constructing the almost unbiased fourth-order cumulant matrices. The SNR is set to be 10 dB. In Fig. 4(a), nine sources uniformly distributed from $-60°$ to $60°$ with their range parameters $\{\lambda, 2\lambda, 3\lambda, 4\lambda, +\infty, +\infty, +\infty, +\infty, +\infty\}$ are considered. From Fig. 4(a), we can ensure that the proposed algorithm can estimate $2N + 2MN - M - 2$ sources effectively via an array of $2M + 2N - 1$ sensors. In Fig. 4(b), we decrease the number of sources to seven, but make two of them closely spaced ($5°$ separation). It can be clearly observed that our algorithm also resolve them well.

In the second experiment, we show the spatial spectrum obtained by the proposed algorithm in DOA and range domain, respectively. The range grid for far-field sources r_F is set to be 80λ. The SNR and the number of snapshots are fixed at 10 dB and 10000, respectively. In Figs. 5(a) and 5(b), three sources with distinct DOAs are considered, whose locations are set to be $\{\theta_1 = -10°, r_1 = 2\lambda\}$, $\{\theta_2 = 30°, r_2 = 4\lambda\}$, $\{\theta_3 = 50°, r_3 = +\infty\}$, respectively. From the simulation results, we can clearly find that there are two near-field sources and one far-field source impinging on

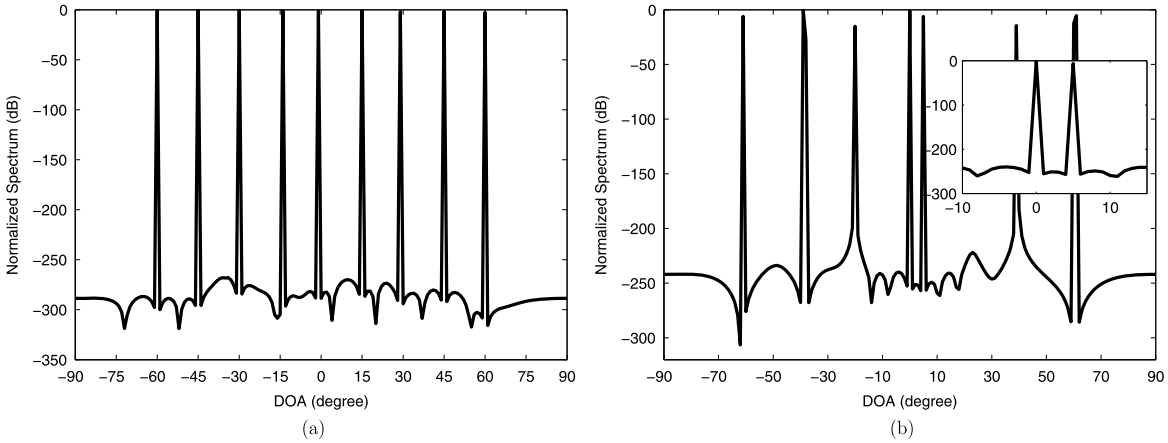

Fig. 4. Normalized spatial spectrum obtained using the proposed algorithm with 10 dB SNR and 10000 snapshots. (a) Nine well separated sources. (b) Seven sources with two of them closely spaced.

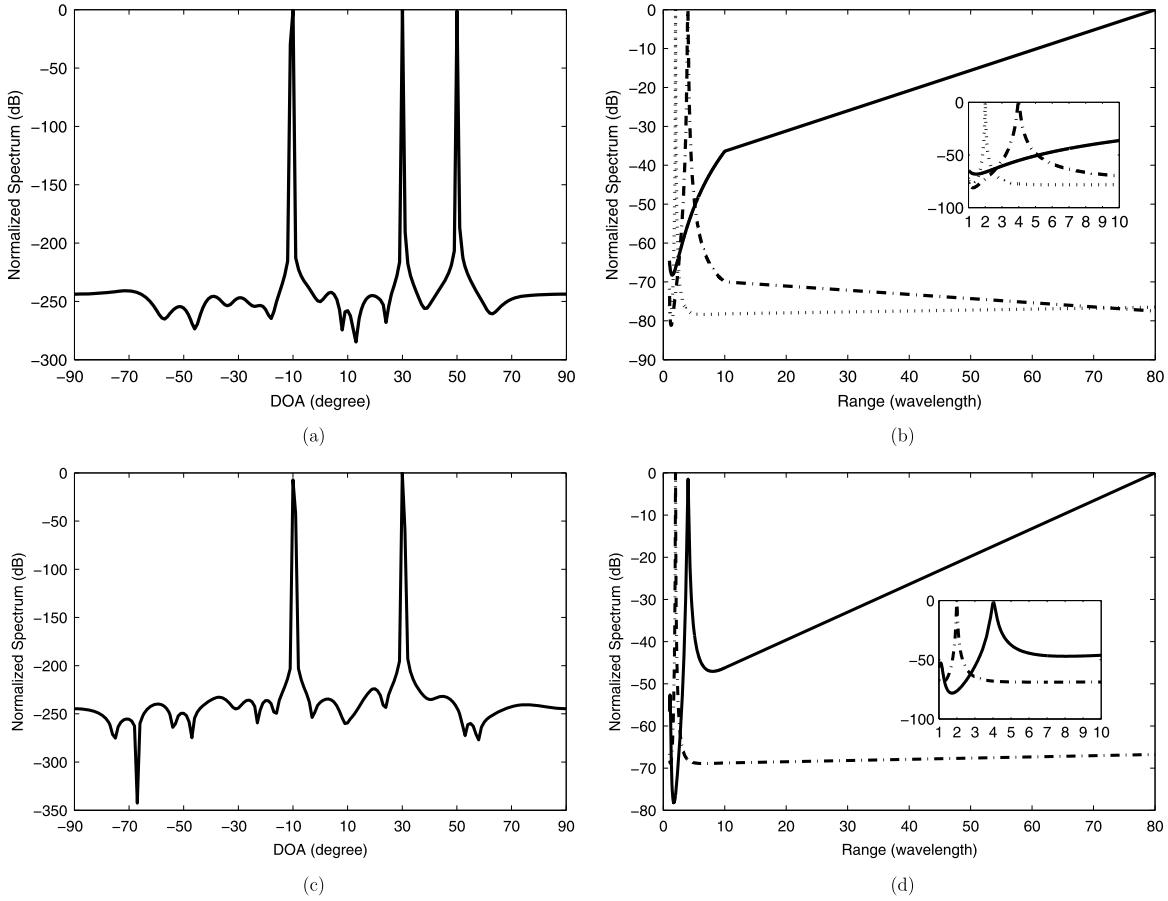

Fig. 5. Normalized spatial spectrum in DOA and range domain with 10 dB SNR and 10000 snapshots. (a) and (b) for three sources with distinct DOAs; (c) and (d) for one near-field source and one far-field source with same DOA.

the array. In Figs. 5(c) and 5(d), the locations of three sources are same with Figs. 5(a) and 5(b) except that the second source and the third source have the same DOA, i.e., $\theta_2 = \theta_3 = 30°$. Although the spectrum of DOA has only two peaks, the corresponding spectrum of range has three peaks, two of them are obtained by using $\hat{\theta} = 30°$, one peak is located at near-field region (or Fresnel region), and the other is located at far-field region (far beyond the Fresnel region), which indicates that there exist one near-field source and one far-field source impinging on the array with same DOA. This simulation validates the high efficiency of the proposed algorithm on classifying the source types.

In the third experiment, we compare the probability of separation of different algorithms against SNR and the angle separation, whose curves are plotted in Figs. 6(a) and 6(b), respectively. In Fig. 6(a), two sources located at $\{\theta_1 = 10°, r_1 = 4\lambda\}$, $\{\theta_2 = 13°, r_2 = +\infty\}$ are considered, and SNR varies from -5 dB to 20 dB in 5 dB-steps. While in Fig. 6(b), the θ_1 is fixed at 10°, whereas θ_2 varies from 12° to 26° in steps of 2°, and SNR = 5 dB. By definition, the two sources are resolved in the DOA domain if both the bias of two sources do not exceed 1°. From the simulation result, we observe that the proposed algorithm can resolve closely spaced

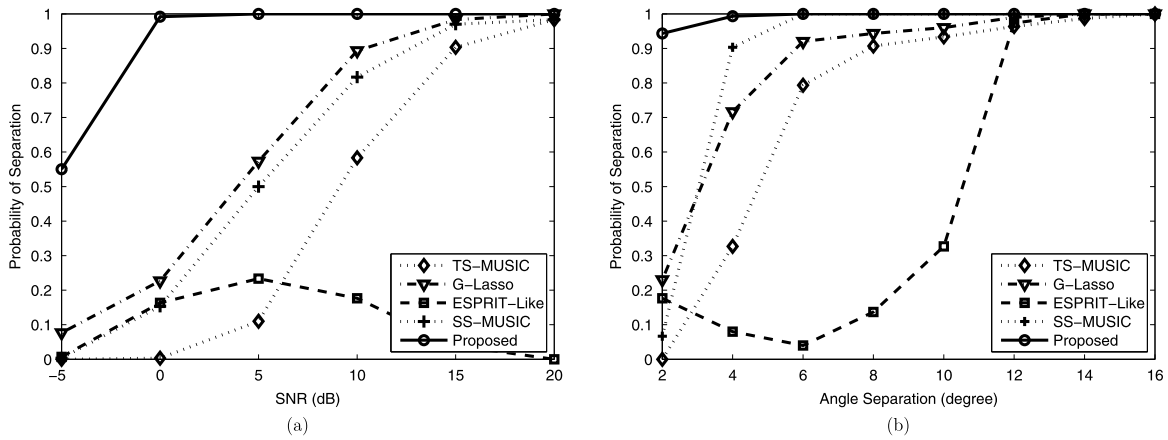

Fig. 6. Probability of separation against SNR and the angle separation. (a) Against SNR with 10000 snapshots and 3° separation; (b) Against angle separation with 5 dB SNR and 10000 snapshots.

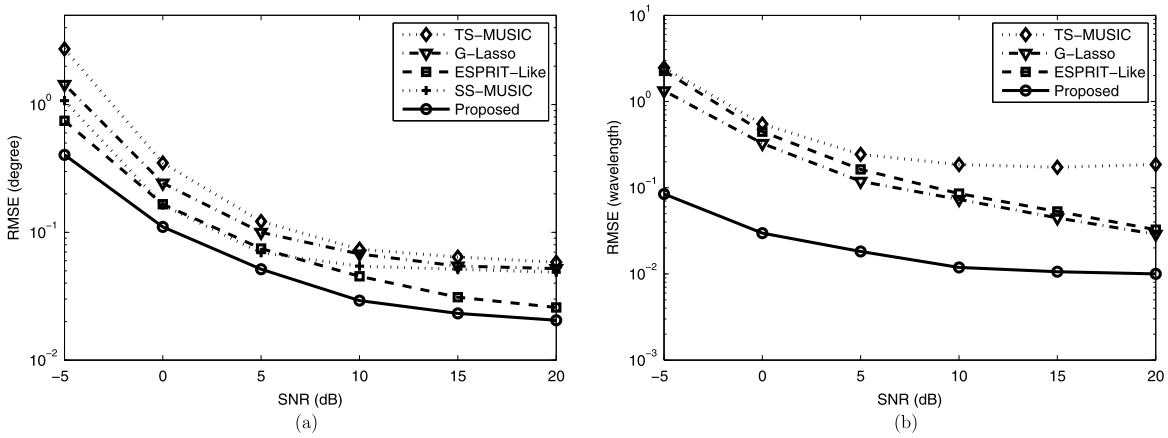

Fig. 7. RMSE of DOA and range estimations versus SNR with 10000 snapshots. (a) RMSE of DOA estimations; (b) RMSE of range estimations.

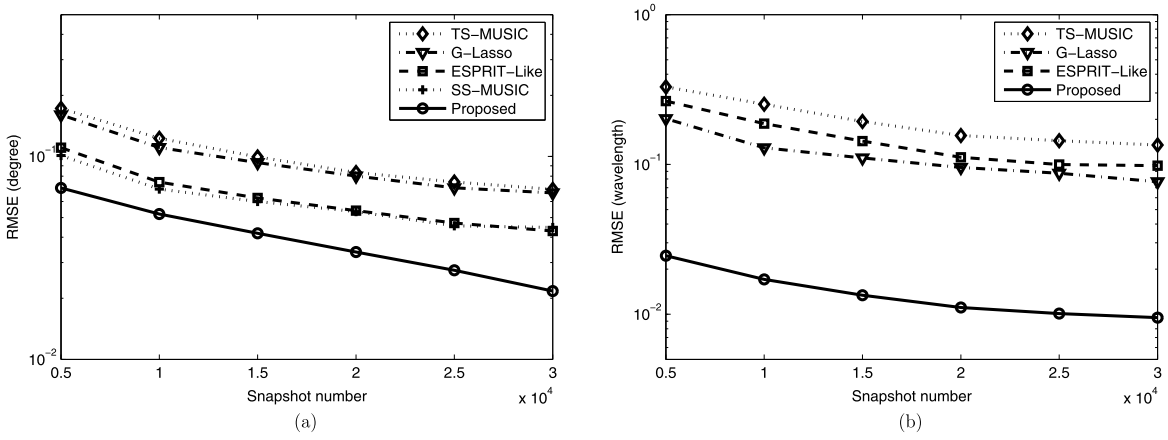

Fig. 8. RMSE of DOA and range estimations versus the number of snapshots with 5 dB SNR. (a) RMSE of DOA estimations; (b) RMSE of range estimations.

sources with lower SNR and smaller angle separation in comparison with previous algorithms.

In the last experiment, we evaluate the RMSE of DOA and range estimations in different SNRs and different number of snapshots. The corresponding results are shown in Figs. 7 and 8, respectively. Two well-separated sources including one near-field source and one far-field source are located at $\{\theta_1 = -20°, r_1 = 4\lambda\}$, $\{\theta_2 = 30°, r_2 = +\infty\}$. In Fig. 7, we vary the SNR from -5 dB to 20 dB with 10000 snapshots. While in Fig. 8, we fix the SNR to be 5 dB, and vary the number of snapshots from 5000 to 30000 in steps of 5000. The simulation results show that the proposed algorithm outperforms the compared algorithms greatly. This improved performance can be explained as follows: i) For DOA estimation, much higher number of effective consecutive lags is utilized; ii) For range estimation, much more fourth-order cumulant data is exploited.

5. Conclusion

In this paper, we present a new algorithm to solve mixed near-field and far-field source localization problem. Instead of using

generalized uniform linear array, a symmetric nested array structure is adopted. By constructing a fourth-order cumulant matrix of properly chosen the sensor output of SNA, the effective number of consecutive lags is increased greatly. And then, the CS-based technique is utilized to fully use this increased consecutive lags, and successively obtain DOA estimation of all sources. By arranging the cumulant elements in an appropriate manner, anther fourth-order cumulant matrix that related to both DOA and range parameters is obtained. Further, the source types are classified and the range of near-field sources is achieved via 1-D spectral searching. The proposed algorithm shows several salient advantages, such as increased resolution, improved estimation accuracy and estimating more sources with less sensors. Performance analysis and simulation results verify the superiority of the proposed algorithm.

Acknowledgments

This work was supported in part by the National Natural Science Foundation of China under Grants 61601398, 61471313, in part by the Young Talent Program of Colleges in Hebei Province under Grant BJ2016051, and in part by the CETC Key Laboratory of Aerospace Information Applications Cooperative Technology Project under Grant EX166290016.

References

[1] R.O. Schmidt, Multiple emitter location and signal parameter estimation, IEEE Trans. Antennas Propag. 34 (3) (1986) 276–280.
[2] R. Roy, T. Kailath, ESPRIT-estimation of signal parameters via rotational invariance techniques, IEEE Trans. Acoust. Speech Signal Process. 37 (7) (1989) 984–995.
[3] N. Guzey, H. Xu, S. Jagannathan, Localization of near-field sources in spatially colored noise, IEEE Trans. Instrum. Meas. 64 (8) (2015) 2302–2311.
[4] D. Starer, A. Nehorai, Passive localization of near-field sources by path following, IEEE Trans. Signal Process. 42 (1994) 677–680.
[5] J. Volakis, Antenna Engineering Handbook, fourth edition, McGraw-Hill, 2009, pp. 1–7.
[6] G. Arslan, F.A. Sakarya, B.L. Evans, Speaker localization for far-field and near-field wideband sources using neural networks, in: Proc. IEEE-EURASIP Workshop on Nonlin. Signal Image Process., Antalya, Turkey, 1999, pp. 528–532.
[7] S. Argentieri, P. Danes, P. Soueres, Modal analysis based beamforming for nearfield or farfield speaker localization in robotics, in: Proc. 2006 IEEE Int. Conf. Robots Syst., 2006, pp. 866–871.
[8] M. Agrawah, R. Abrahamsson, P. Ahgren, Optimum beam-forming for a nearfield source in signal correlated interferences, Signal Process. 86 (5) (2006) 915–923.
[9] J. Liang, D. Liu, Passive localization of mixed near-field and far-field sources using two-stage music algorithm, IEEE Trans. Signal Process. 58 (1) (2010) 108–120.
[10] B. Wang, J. Liu, X. Sun, Mixed sources localization based on sparse signal reconstruction, IEEE Signal Process. Lett. 19 (8) (2012) 487–490.
[11] Y. Tian, X. Sun, Mixed sources localisation using a sparse representation of cumulant vectors, IET Signal Process. 8 (6) (2014) 606–611.
[12] K. Wang, L. Wang, J. Shang, X. Qu, Mixed near-field and far-field sources localization based on uniform linear array partition, IEEE Sens. J. (2016), https://doi.org/10.1109/JSEN.2016.2603182.
[13] J. He, M.N.S. Swamy, M.O. Ahmad, Efficient application of MUSIC algorithm under the coexistence of far-field and near-field sources, IEEE Trans. Signal Process. 60 (4) (2012) 2066–2070.
[14] G. Liu, X. Sun, Spatial differencing method for mixed far-field and near-field source localization, IEEE Signal Process. Lett. 21 (11) (2014) 1331–1335.
[15] S. Pillai, Array Signal Processing, Springer, New York, NY, USA, 1989.
[16] R.T. Hoctor, S.A. Kassam, The unifying role of the co-array in aperture synthesis for coherent and incoherent imaging, Proc. IEEE 78 (1990) 735–752.
[17] P. Pal, P.P. Vaidyanathan, Nested array: a novel approach to array processing with enhanced degrees of freedom, IEEE Trans. Signal Process. 58 (8) (2010) 4167–4181.
[18] P.P. Vaidyanathan, P. Pal, Sparse sensing with co-prime samplers and arrays, IEEE Trans. Signal Process. 59 (2) (2011) 573–586.
[19] Y.D. Zhang, Q. Sia, M.G. Amin, Near-field source localization based on sparse reconstruction of sensor-angle distributions, in: Proc. IEEE Radar, 2015, pp. 891–895.
[20] K.R. Dandekar, H. Ling, G. Xu, Experimental study of mutual coupling compensation in smart antenna applications, IEEE Trans. Wirel. Commun. 1 (3) (2002) 480–487.
[21] H.T. Hui, An effective compensation method for the mutual coupling effect in phased arrays for magnetic resonance imaging, IEEE Trans. Antennas Propag. 53 (11) (2005) 3576–3583.
[22] Q. Shen, W. Liu, W. Cui, S. Wu, Extension of nested array with the fourth-order difference co-array enhancement, in: Proc. 2016 IEEE Int. Conf. Acoust., Speech and Signal Process., 2016, pp. 2991–2995.
[23] M.C. Dogan, J.M. Mendel, Applications of cumulants to array processing-Part I: aperture extension and array calibration, IEEE Trans. Signal Process. 43 (1995) 1200–1216.
[24] R. Tibshirani, Regression shrinkage and selection via the Lasso, J. R. Stat. Soc. 58 (2) (1996) 267–288.
[25] P.C. Hansen, D.P. O'Leary, The use of the L-curve in the regularization of discrete ill-posed problems, SIAM J. Sci. Comput. 14 (6) (1993) 1487–1503.
[26] J. Sturm, Using SeDuMi 1.02: a MATLAB toolbox for optimization over symmetric cones, Optim. Methods Softw. 11 (1–4) (1999) 625–653.
[27] M. Grant, S. Boyd, CVX: Matlab software for disciplined convex programming, version 2.0 beta, build 1023. [Online]. Available: http://cvxr.com/cvx.
[28] P. Pal, P.P. Vaidyanathan, Coprime sampling and the MUSIC algorithm, presented at IEEE Digit. Signal Process. Workshop, 2011.
[29] D. Donoho, M. Elad, Optimally sparse representation in general (nonorthogonal) dictionaries via ℓ_1 minimation, in: Proc. Nation. Acad. Scien., December 2003, pp. 2197–2202.
[30] C.L. Liu, P.P. Vaidyanathan, Cramér–Rao bounds for coprime and other sparse arrays, which find more sources than sensors, Digit. Signal Process. 61 (2017) 43–61.
[31] A. Koochakzadeh, P. Pal, Cramér–Rao bounds for underdetermined source localization, IEEE Signal Process. Lett. 23 (7) (2016) 919–923.
[32] Z.Q. He, Z.P. Shi, L. Huang, Covariance sparsity-aware DOA estimation for nonuniform noise, Digit. Signal Process. 28 (1) (2014) 75–81.

Ye Tian received the Ph.D. degree in Communication Engineering from Jilin University, Changchun, China, in 2014. Currently, he is an Associate Professor in School of Information Science and Technology, Yanshan University. His research interests include array signal processing, sparse signal representation and phase retrieval.

Qiusheng Lian received the Ph.D. degree in Yanshan University, in 2006. He is currently a Professor of School of Information Science and Technology at Yanshan University, China. His current research interests include dictionary learning, phase retrieval and nonlinear compressed sensing.

He Xu received the B.S. and M.S. degrees in Communication Engineering from Jilin University, Changchun, China, in 2010 and 2013, respectively. His current research interests include array signal processing, compressed sensing and their applications in radar.